

# Cooperative Loading and Release Behavior of a Metal–Organic Receptor

Quan Gan,<sup>†</sup> Tanya K. Ronson,<sup>†</sup> David A. Vosburg,<sup>‡</sup> John D. Thoburn,<sup>§</sup> and Jonathan R. Nitschke<sup>\*,†</sup>

<sup>†</sup>Department of Chemistry, University of Cambridge, Lensfield Road, Cambridge CB2 1EW, United Kingdom

<sup>‡</sup>Department of Chemistry, Harvey Mudd College, 301 Platt Boulevard, Claremont, California 91711, United States

<sup>§</sup>Department of Chemistry, Randolph-Macon College, 204 Henry Street, Ashland, Virginia 23005, United States

**S** Supporting Information

**ABSTRACT:** In order to design artificial chemical systems that are capable of achieving complex functions, it is useful to design synthetic receptors that mimic their biological counterparts. Biological functions are underpinned by properties that include specific binding with high affinity and selectivity, cooperativity, and release triggered by external stimuli. Here we show that a metal–organic receptor constructed through subcomponent self-assembly can selectively and cooperatively load and release oxocarbon anions. The flexible coordination spheres of its cadmium(II) centers allow the receptor to dynamically adjust its structure upon exchanging four triflate or triflimide counterions for two oxocarbon anions, resulting in strong cooperativity and very tight binding, with an apparent association constant for  $C_5O_5^{2-}$  of  $5 \times 10^{10} M^{-1}$ . Substituting the cadmium(II) ions for copper(I) by switching solvent prompted a structural reorganization and release of the oxocarbon anions. Its cooperative behavior allows the receptor to carry a greater payload than would be possible in a noncooperative analogue.

The cooperative binding and release of substances in response to external stimuli is a key feature of metabolic and signaling functions in biological systems.<sup>1</sup> A canonical example is the dioxygen transport protein hemoglobin, where dioxygen binding at one of the four sites increases the oxygen affinity of the other sites, resulting in efficient delivery of oxygen from respiratory organs to tissues where it is needed.<sup>2</sup> This cooperative behavior enables hemoglobin to deliver 1.7 times more oxygen than would be possible if the binding sites were noncooperative.<sup>3</sup> The cooperative loading phenomenon in natural biomacromolecules has inspired the study of smaller synthetic analogues, both to better understand the mechanisms involved in natural systems and to develop functional systems that may benefit from such binding interactions. Several groups have fruitfully investigated artificial guest catch-and-release molecular systems,<sup>4</sup> including both open architectures and closed capsules, as well as demonstrating artificial cooperative binding behavior.<sup>5</sup> The present work builds upon these foundations by demonstrating a receptor that is capable of not only cooperative, selective uptake<sup>6</sup> but also controlled, complete release under well-defined conditions.

Subcomponent **A**, based on a pseudo-four-fold symmetric (cyclopentadienyl)(cyclobutadienyl) cobalt (CpCoCb) moiety,

was designed and synthesized based on literature precedent for related molecules.<sup>7</sup> Four anilines provide four “arms” to react with 2-formylpyridines, generating a tetrakis(bidentate) ligand. Meta-substituted anilines were chosen to bring the ligand arms close enough to form a sandwich structure through free rotation between the anilines and the *para*-phenylene rings (Figure 1). Symmetrical sandwich structure **1** formed during

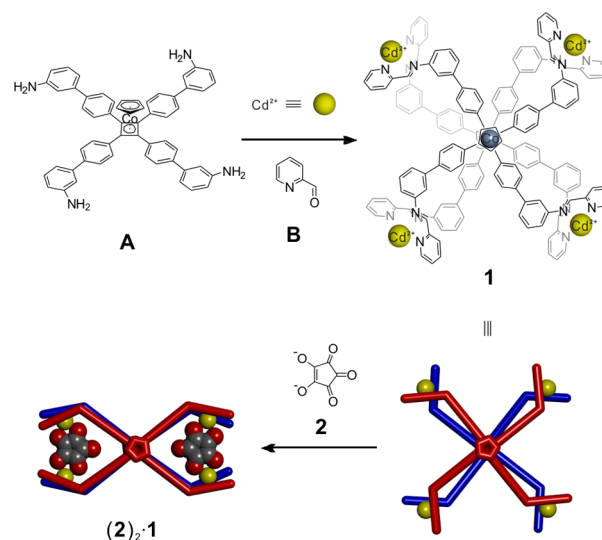


**Figure 1.** Synthesis and schematic representation of metal–organic receptor **1** and a (2)<sub>2</sub>·**1** complex. The reaction of **A** (2 equiv) and **B** (8 equiv) with Cd<sup>2+</sup> (4 equiv) led to the formation of **1**. Addition of croconate anion (**2**) to **1** gave rise to a (2)<sub>2</sub>·**1** complex.

the reaction of **A** with Cd<sup>II</sup> and 2-formylpyridine **B** in a 2:4:8 ratio in acetonitrile. NMR and ESI-MS spectra of **1** were consistent with the formation of a highly symmetric M<sub>4</sub>L<sub>2</sub> assembly in quantitative yield (Figures S1–S4).

The crystal structure of **1**·(NTf<sub>2</sub>)<sub>8</sub> was consistent with the approximate D<sub>4</sub> symmetry observed in solution by NMR, in which two ligands are brought together by formation of coordination bonds, with the Cp rings on the exterior faces of the complex (Figure 2a,b). Each ligand coordinates to four Cd<sup>II</sup> ions, with an average distance of 16.5 Å between adjacent metal centers. Each Cd<sup>II</sup> is bound by a pyridyl-imine “arm” from each

Received: November 25, 2014

Published: January 23, 2015

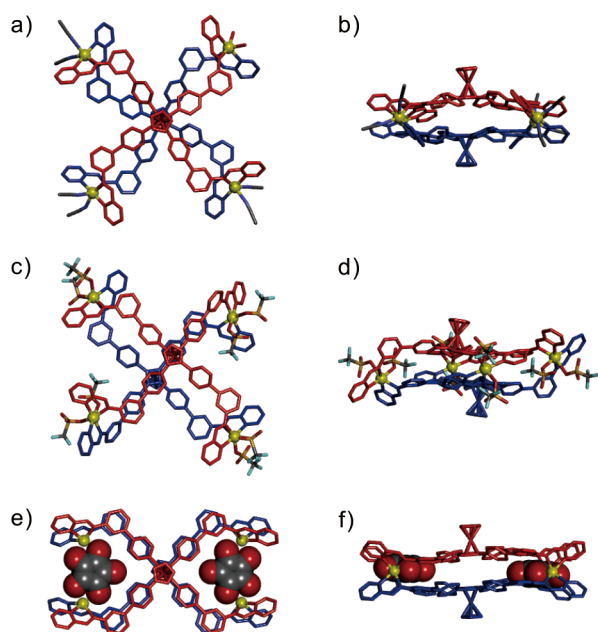


**Figure 2.** Top and side views of the crystal structures of  $1 \cdot (\text{NTf}_2)_8$  (a and b),  $1 \cdot (\text{OTf})_8$  (c and d), and  $(2)_2 \cdot 1$  complex (e and f). Oxocarbons are shown as CPK representations (C, gray; O, red). Hydrogen atoms, uncoordinated counterions, solvent molecules, and disorder have been omitted for clarity.<sup>14</sup>

ligand, leaving two free coordination sites that are occupied by acetonitrile or water to complete the octahedral coordination sphere of  $\text{Cd}^{\text{II}}$ .

The crystal structure of  $1 \cdot (\text{OTf})_8$  (Figure 2c,d), in contrast, possesses  $C_i$  symmetry, in which two opposing corners are similar to those of  $1 \cdot (\text{NTf}_2)_8$ , with the two pyridyl donors occupying *trans* coordination sites. The other two  $\text{Cd}^{\text{II}}$  centers adopt a less symmetric coordination geometry, having pyridyl donors *cis* to each other. The two central cyclobutadienyl rings, which are stacked atop each other in  $1 \cdot (\text{NTf}_2)_8$  (centroid–centroid distance 4.5 Å), adopt a slipped, offset arrangement in  $1 \cdot (\text{OTf})_8$  (centroid–centroid distance 5.3 Å).

NMR measurements in solution provided evidence for the presence of two configurations of **1** for both the triflimide and triflate salts, with symmetries consistent with the two forms observed in the solid state. The triflimide salt was used in all of our solution studies due to the greater solubility of the resultant complexes in  $\text{CD}_3\text{CN}$ . At 278 K, NMR data were consistent with a  $D_4$ -symmetric structure, whereas a second set of signals appeared when the temperature was increased to 333 K (Figure S5). We infer the new species to be the  $C_i$ -symmetric conformer of **1**, since it possesses twice as many resonances as the major  $D_4$ -symmetric species. Diffusion-ordered  $^1\text{H}$  NMR spectroscopy (DOSY) was also consistent with the two species having similar sizes (Figure S7). The enthalpy and entropy of transformation from the  $D_4$  to  $C_i$  isomer in acetonitrile were determined from a van 't Hoff plot to be  $6.7 \text{ kJ mol}^{-1}$  and  $4.5 \text{ J mol}^{-1} \text{ K}^{-1}$ , respectively (Figure S6). The positive values of both  $\Delta H$  and  $\Delta S$  illustrate that the  $D_4$  symmetric conformation of receptor **1** is enthalpically preferred while the  $C_i$  conformation is favored entropically. We attribute the dynamic behavior of compound **1** to the flexible coordination sphere of the large  $\text{Cd}^{\text{II}}$  ions, which allows them to tolerate distorted coordination geometries.<sup>8</sup>

We hypothesized that **1** would be a suitable receptor for anions, whereby the weakly coordinated solvent or anions occupying the two vacant coordination sites at each  $\text{Cd}^{\text{II}}$  center would be displaced by more strongly coordinating anions. Furthermore, we envisaged that the dynamic reconfiguration of **1** might allow it to bind anions cooperatively via rearrangement of the coordination sphere of the metal centers upon addition of a suitable anion. NMR titration experiments of receptor **1** with the tetrabutylammonium salts of croconate ( $\text{C}_5\text{O}_5^{2-}$ , **2**), squarate ( $\text{C}_4\text{O}_4^{2-}$ , **3**) and rhodizionate ( $\text{C}_6\text{O}_6^{2-}$ , **4**) were carried out. In all cases, complexation was inferred to occur, as new signals in the  $^1\text{H}$  NMR spectra emerged, and free receptor signals decreased, consistent with slow exchange between complexed and uncomplexed states on the  $^1\text{H}$  NMR time scale (Figures S8–S10). ESI mass spectra displayed ions corresponding to 1:2 complexes (Figures S16 and S17). During the titration process, we observed two new sets of peaks. One set of signals arose first but then decreased with further anion addition, while the other species gradually increased and remained following saturation; we therefore assigned these to the 1:1 and 1:2 complexes, respectively. DOSY NMR further showed comparable diffusion rates for the two complexes, suggesting that each  $^1\text{H}$  NMR resonance belongs to the framework of an intact  $\text{M}_4\text{L}_2$  receptor rather than to smaller fragments (Figure S13).

Further solution characterization of the complex was hindered by the  $^1\text{H}$  NMR silence of the oxocarbons. The solid-state structure (Figure 2e,f), however, revealed the original  $\text{M}_4\text{L}_2$  architecture with two bound molecules of **2**. Each croconate anion is coordinated in a bridging bis-bidentate manner to two  $\text{Cd}^{\text{II}}$  centers, with an average Cd–O bond length of 2.3 Å. Each  $\text{Cd}^{\text{II}}$  center in  $(2)_2 \cdot 1$  is thus coordinated by two pyridyl-imine ligands and one croconate anion in a trigonal prismatic geometry, in contrast to the distorted octahedral coordination observed in the absence of the guest. Binding of the croconate anions thus induces a structural reorganization of the  $\text{M}_4\text{L}_2$  architecture. The bridging anions bring pairs of  $\text{Cd}^{\text{II}}$  centers closer together, with the Cd···Cd distance shrinking from 16.5 to 7.4 Å, and the “arms” of the receptor become eclipsed in order to reposition the free coordination sites to bind to the anions.

The squarate anion **3** was chosen for UV–vis titration studies as the absorbances of both croconate and rhodizionate overlap with that of receptor **1**. Nonlinear regression analysis<sup>9</sup> of the titration data (Figure S15) based on a 1:2 binding model gave macroscopic binding constants of  $6.3 \pm 0.3 \times 10^4$  and  $7.90 \pm 0.08 \times 10^5 \text{ M}^{-1}$ , respectively, for  $K_1$  and  $K_2$  in the 1:2 complexation of **1** with squarate anion **3** (binding constants averaged from three runs). The ratio of the corresponding microscopic binding constants,  $K_{2\mu}/K_{1\mu} = 50$ , clearly indicates the positive cooperative nature of this complexation and corresponds to a cooperative Gibbs free energy of  $-9.7 \text{ kJ mol}^{-1}$ . The measured apparent association constant ( $K_a$ ) for **3** binding to **1** was calculated to be  $5 \pm 1 \times 10^{10} \text{ M}^{-1}$  (Figure S15), representing an affinity value that is a composite of the two binding events.

The observed high cooperativity may be interpreted to result from an induced-fit process during recognition:<sup>10</sup> when one oxocarbons docks into the receptor, displacing and exchanging for the less-well-bound counteranions, a conformational change is induced to fit the oxocarbons. The remaining binding site is thereby preorganized to have increased affinity for a second anion. The crystal structures

provide insight as to how this process might occur. A key point is that the staggered “arms” of the receptor become eclipsed following the binding of the first croconate. This eclipsing brings the other two arms of the complex together to bind the second croconate with high affinity.

The cooperative binding observed for squarate also occurred for croconate and rhodizonate. For each of these oxocarbon anions, the intermediate 1:1 complexes were never significantly populated during NMR titration experiments. Among these anions, croconate **2** bound most tightly to **1**, as inferred from NMR experiments where two anions were allowed to compete to bind (Figure S11); croconate was thus chosen for subsequent studies. The binding of receptor **1** with other anions was tested, but the cooperative binding behavior seen for **2–4** was not observed in the cases of  $\text{PF}_6^-$ ,  $\text{BF}_4^-$ ,  $\text{Br}^-$ , or  $\text{I}^-$  (Figure S12).

Having established cooperative loading of anions into **1**, we sought to release the anions completely without disturbing the overall structure. For this purpose the  $\text{Cu}^{\text{I}}_4\text{L}_2$  analogue **5** of  $\text{Cd}^{\text{II}}_4\text{L}_2$  receptor **1** was synthesized and studied (Figure S18). Unlike receptor **1**, each  $\text{Cu}^{\text{I}}$  metal center in complex **5** is fully saturated by two pyridyl-imine ligands, since  $\text{Cu}^{\text{I}}$  ions favor a tetrahedral coordination environment; the metal centers of **5** thus exhibited no tendency to coordinate anions. Upon the addition of excess croconate (4 equiv) to **5**, no new peaks or shifts in the signals were observed in either  $\text{DMSO}-d_6$  or  $\text{CD}_3\text{CN}$  by  $^1\text{H}$  NMR (Figure S21). Further addition of croconate resulted in broadened signals and precipitation of **5** due to anion exchange.

When both  $\text{Cu}^{\text{I}}$  and  $\text{Cd}^{\text{II}}$  were present, we found that **1** and **5** interconverted upon variation of the solvent: complex **1** was preferred in acetonitrile, whereas **5** dominated in DMSO. As a result, **5** could be obtained by adding  $\text{Cu}^{\text{I}}$  to **1** in DMSO, and **5** could be converted into **1** via addition of  $\text{Cd}^{\text{II}}$  in acetonitrile. We infer the stronger solvation of free  $\text{Cd}^{\text{II}}$  by DMSO, and  $\text{Cu}^{\text{I}}$  by acetonitrile, to drive the solvent-dependent metal exchange that allows **1** and **5** to interconvert. The combination of different solvent stability and differential oxocarbon anion recognition ability allows us to envisage a cycle of loading and release of anions by solvent-mediated interconversion between **1** and **5**. The sequence of steps is shown in Figure 3: (i) To an acetonitrile solution of receptor **1** containing free  $\text{Cu}^{\text{I}}$  (4 equiv) was added anion **2** (2.4 equiv), leading to formation of the  $(2)_2\cdot 1$  complex, i.e., anion loading. (ii) Addition of DMSO stimulated the replacement of the  $\text{Cd}^{\text{II}}$  ions of the complex with  $\text{Cu}^{\text{I}}$  ions, resulting in transformation of **1** into **5** and thus release of the 2 equiv of **2**. (iii) Addition of diethyl ether to the above solution followed by filtration of the precipitated **5** allowed its separation from the released **2** and  $\text{Cd}^{\text{II}}$  remaining in solution. (iv) Finally, complex **5** transformed back into receptor **1** following dissolution of the precipitate in acetonitrile and the subsequent addition of  $\text{Cd}^{\text{II}}$  (4 equiv). Each conversion step was monitored by  $^1\text{H}$  NMR (Figure 4).

This cycle implements a strategy of cooperative catch and release of an anion in two different environments through altering the properties of the receptor upon addition of chemical stimuli. The considerable manipulation of compounds and solutions required by this strategy would be most worthwhile in the context of high-value extractions, as in the removal of sulfate from nuclear waste.<sup>11</sup>

The addition of  $\text{Cu}^{\text{I}}$  to an acetonitrile/DMSO solution of  $(2)_2\cdot 1$  (Figure S22) resulted in its clean conversion to **5** and free **2**, without forming  $\text{Cu}^{\text{I}}-\text{Cd}^{\text{II}}$  hybrid structures. This

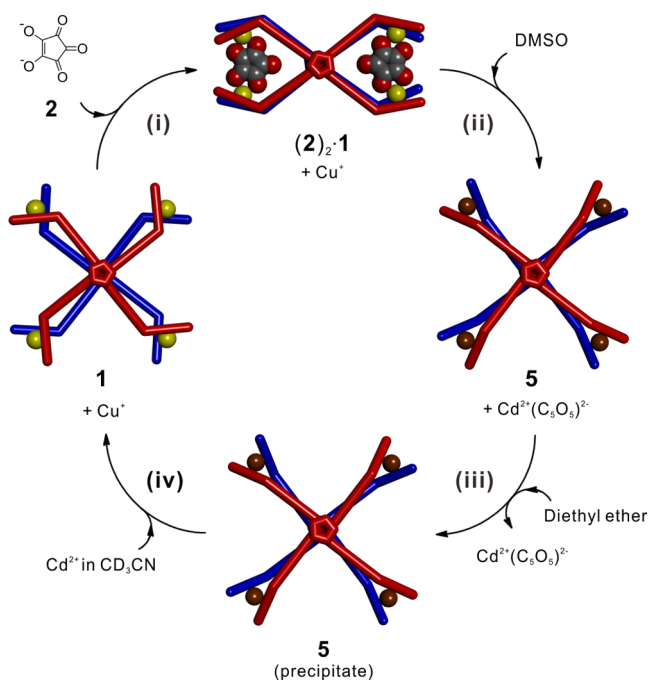


**Figure 3.** Schematic representation of loading and release of croconate with receptors **1** and **5** by switching the metal centers. (i) Trapping **2** as  $(2)_2\cdot 1$ . (ii) DMSO addition prompted metal exchange and release of anion **2**. (iii) Addition of diethyl ether gave solid complex **5**, with  $\text{Cd}^{2+}\cdot 2$  in the filtrate. (iv) Redissolution of **5** in  $\text{CD}_3\text{CN}$  followed by addition of  $\text{Cd}^{2+}$  regenerated the initial state.

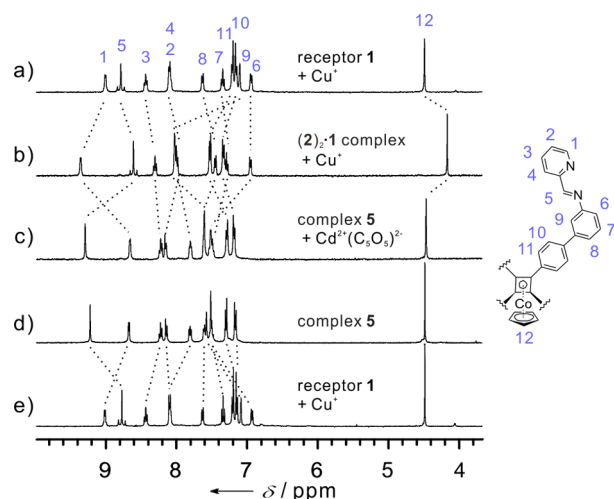


**Figure 4.** Partial  $^1\text{H}$  NMR spectra (400 MHz, 298 K) of the catch and release of anions following the cycle of Figure 3. (a) Receptor **1**· $(\text{NTf}_2)_8$  (0.25 mM) with  $\text{Cu}^{\text{I}}$  (4 equiv) in  $\text{CD}_3\text{CN}$  (500  $\mu\text{L}$ ); (b) addition of **2** (2.4 equiv) to solution a; (c) addition of  $\text{DMSO}-d_6$  (50  $\mu\text{L}$ ) to solution b; (d) precipitate obtained from addition of diethyl ether to c following dissolution in  $\text{CD}_3\text{CN}$  (500  $\mu\text{L}$ ); (e) addition of  $\text{Cd}^{2+}$  (4 equiv) to solution d.

observation suggests that both metal substitution and anion release are strongly cooperative. If the metal substitution process was not cooperative, partially exchanged receptor signals would be significant and would greatly complicate the NMR spectra. Interestingly, in the absence of oxocarbon anions, complicated spectra were observed during metal substitution (Figure S23), which we attribute to mixed-metal complexes.

The observed high-affinity cooperative catch and release behavior provides **1** with advantages in comparison with other artificial systems in which no cooperativity occurs.<sup>5–12</sup> At a concentration of  $5.0 \times 10^{-6}$  M, **1** would be half-saturated with **3** at an anion concentration of  $8.0 \times 10^{-6}$  M. In the absence of cooperativity, however, the hypothetical maximum amount of anion that could be loaded under the same conditions is  $3.1 \times 10^{-6}$  M. Thus, the cooperative binding behavior of the receptor enables it to deliver 1.6 times as much anion as it would if the sites were independent, a value comparable to the cooperative advantage enjoyed by hemoglobin in transporting oxygen.<sup>4</sup> Furthermore, **1** efficiently catches and releases anions at low concentrations within a narrow response region, where small changes in conditions lead to a complete transformation between free and bound states. These features are of considerable benefit in the context of chemical sensors<sup>12</sup> or drug delivery systems.<sup>13</sup> Although we did not carry out studies on a sufficiently large scale to allow yield determination, NMR spectra did not show substantial impurity buildup (estimated <5%) even after four turns around the cycle of Figure 3. This observation is consistent with an efficient strategy.

In summary, we have shown how oxocarbon anions can be cooperatively loaded and released by regulating the properties of an artificial receptor. The binding of the first oxocarbon anion to receptor **1** increases the binding affinity of the second one, while both are released completely in the reverse process triggered by chemical stimuli (switching the solvent resulting in exchanging the metal center). This system also illustrates induced-fit recognition behavior: the flexibility of the arms of the complex allows dynamic adjustment of its binding sites via rearrangement of the metal coordination geometry to cooperatively accommodate anions with high affinity.

## ■ ASSOCIATED CONTENT

### Supporting Information

Full experimental procedures, NMR and ESI-MS spectra, X-ray crystallographic data including CIF files (also deposited with the Cambridge Crystallographic Data Centre as entries CCDC 1012306–1012309). This material is available free of charge via the Internet at <http://pubs.acs.org>.

## ■ AUTHOR INFORMATION

### Corresponding Author

\*jrn34@cam.ac.uk

### Notes

The authors declare no competing financial interest.

## ■ ACKNOWLEDGMENTS

This work was supported by the Marie Curie Academic-Industrial Initial Training Network on Dynamic Molecular Nanostructures (DYNAMOL) of the European Union's Seventh Framework Programme (FP7) and the U.K. Engineering and Physical Sciences Research Council (EPSRC). We thank Diamond Light Source (U.K.) for synchrotron beam time on I19 (MT8464), the EPSRC National Crystallography Service for X-ray data collection, and the EPSRC Mass Spectrometry Service at Swansea for high-resolution ESI experiments.

## ■ REFERENCES

- (1) (a) Whitty, A. *Nat. Chem. Biol.* **2008**, *4*, 435. (b) Hunter, C. A.; Anderson, H. L. *Angew. Chem., Int. Ed.* **2009**, *48*, 7488.
- (2) Perutz, M. F. *Q. Rev. Biophys.* **1989**, *22*, 139.
- (3) *Biochemistry*; Berg, J. M.; Tymoczko, J. L.; Stryer, L., Eds.; W. H. Freeman: New York, 2002.
- (4) (a) Han, M.; Michel, R.; He, B.; Chen, Y. S.; Stalke, D.; John, M.; Clever, G. H. *Angew. Chem., Int. Ed.* **2013**, *52*, 1319. (b) Kishi, N.; Akita, M.; Kamiya, M.; Hayashi, S.; Hsu, H.-F.; Yoshizawa, M. *J. Am. Chem. Soc.* **2013**, *135*, 12976. (c) Hiraoka, S.; Harano, K.; Shiro, M.; Shionoya, M. *Angew. Chem., Int. Ed.* **2005**, *44*, 2727. (d) Duroola, F.; Rebek, J. *Angew. Chem., Int. Ed.* **2010**, *49*, 3189. (e) Pochorowski, I.; Ebert, M.-O.; Gisselbrecht, J.-P.; Boudon, C.; Schweizer, W. B.; Diederich, F. *J. Am. Chem. Soc.* **2012**, *134*, 14702. (f) Lewis, J. E.; Gavey, E. L.; Cameron, S. A.; Crowley, J. D. *Chem. Sci.* **2012**, *3*, 778. (g) Hua, Y.; Flood, A. H. *J. Am. Chem. Soc.* **2010**, *132*, 12838. (h) Schmitt, F.; Freudenreich, J.; Barry, N. P.; Juillerat-Jeanerret, L.; Stüss-Fink, G.; Therrien, B. *J. Am. Chem. Soc.* **2011**, *134*, 754.
- (5) (a) Pistner, A. J.; Lutterman, D. A.; Ghidui, M. J.; Ma, Y.-Z.; Rosenthal, J. *J. Am. Chem. Soc.* **2013**, *135*, 6601. (b) Ikeda, M.; Tanida, T.; Takeuchi, M.; Shinkai, S. *Org. Lett.* **2000**, *2*, 1803. (c) Ikeda, T.; Hirata, O.; Takeuchi, M.; Shinkai, S. *J. Am. Chem. Soc.* **2006**, *128*, 16008. (d) Deutman, A. B.; Monneureau, C.; Moalin, M.; Coumans, R. G.; Veling, N.; Coenen, M.; Smits, J. M.; de Gelder, R.; Elemans, J. A.; Ercolani, G. *Proc. Natl. Acad. Sci. U.S.A.* **2009**, *106*, 10471. (e) Nabeshima, T.; Yoshihira, Y.; Saiki, T.; Akine, S.; Horn, E. *J. Am. Chem. Soc.* **2003**, *125*, 28. (f) Willans, C. E.; Anderson, K. M.; Potts, L. C.; Steed, J. W. *Org. Biomol. Chem.* **2009**, *7*, 2756. (g) Huang, W.-H.; Liu, S.; Zavalij, P. Y.; Isaacs, L. *J. Am. Chem. Soc.* **2006**, *128*, 14744. (h) Park, J. S.; Le Derf, F.; Bejger, C. M.; Lynch, V. M.; Sessler, J. L.; Nielsen, K. A.; Johnsen, C.; Jeppesen, J. O. *Chem.—Eur. J.* **2010**, *16*, 848. (i) Sato, H.; Tashiro, K.; Shinmori, H.; Osuka, A.; Murata, Y.; Komatsu, K.; Aida, T. *J. Am. Chem. Soc.* **2005**, *127*, 13086. (j) Takezawa, H.; Murase, T.; Resnati, G.; Metrangolo, P.; Fujita, M. *J. Am. Chem. Soc.* **2014**, *136*, 1786. (k) Jiang, W.; Nowosinski, K.; Löw, N. L.; Dzyuba, E. V.; Klautzsch, F.; Schäfer, A.; Huuskonen, J.; Rissanen, K.; Schalley, C. A. *J. Am. Chem. Soc.* **2012**, *134*, 1860.
- (6) (a) Kremer, C.; Lützen, A. *Chem.—Eur. J.* **2013**, *19*, 6162. (b) Chakrabarty, R.; Mukherjee, P. S.; Stang, P. J. *Chem. Rev.* **2011**, *111*, 6810.
- (7) Harrison, R. M.; Brotin, T.; Noll, B. C.; Michl, J. *Organometallics* **1997**, *16*, 3401.
- (8) Meng, W.; Ronson, T. K.; Clegg, J. K.; Nitschke, J. R. *Angew. Chem., Int. Ed.* **2013**, *52*, 1017.
- (9) Thordarson, P. *Chem. Soc. Rev.* **2011**, *40*, 1305.
- (10) Koshland, D. E., Jr. *Angew. Chem., Int. Ed.* **1995**, *33*, 2375.
- (11) (a) Custelcean, R.; Remy, P.; Bonnesen, P. V.; Jiang, D.-e.; Moyer, B. A. *Angew. Chem., Int. Ed.* **2008**, *47*, 1866. (b) Custelcean, R.; Bonnesen, P. V.; Duncan, N. C.; Zhang, X.; Watson, L. A.; Van Berkel, G.; Parson, W. B.; Hay, B. P. *J. Am. Chem. Soc.* **2012**, *134*, 8525.
- (12) Vajpayee, V.; Song, Y. H.; Lee, M. H.; Kim, H.; Wang, M.; Stang, P. J.; Chi, K. W. *Chem.—Eur. J.* **2011**, *17*, 7837.
- (13) Su, X.; Aprahamian, I. *Chem. Soc. Rev.* **2014**, *43*, 1963.
- (14) Coles, S. J.; Gale, P. A. *Chem. Sci.* **2012**, *3*, 683.